

A deep learning-based framework for automatic detection of COVID-19 using chest X-ray and CT-scan images

Sivanagireddy Kalli¹, Bukka Narendra Kumar², Saggurthi Jagadeesh¹,
Kushagari Chandramouli Ravi Kumar²

¹Department of Electronics and Communication Engineering, Sridevi Women's Engineering College, Hyderabad, India

²Department of Computer Science and Engineering, Sridevi Women's Engineering College, Hyderabad, India

Article Info

Article history:

Received Aug 7, 2024

Revised Apr 14, 2025

Accepted Jun 8, 2025

Keywords:

Convolutional neural network

COVID-19

CT images

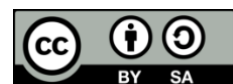
Deep learning

DenseNet-121

ABSTRACT

COVID-19 has profoundly impacted global public health, underscoring the need for rapid detection methods. Radiography and radiologic imaging, especially chest X-rays, enable swift diagnosis of infected individuals. This study delves into leveraging machine learning to identify COVID-19 from X-ray images. By gathering a dataset of 9,000 chest X-rays and CT scans from public resources, meticulously vetted by board-licensed radiologists to confirm COVID-19 presence, the research sets a robust foundation. However, further validation is essential expanding datasets to encompass enough COVID-19 cases enhances convolutional neural network (CNN) accuracy. Among various machine learning techniques, deep learning excels in identifying distinct patterns on imaging characteristics discernible in chest radiographs of COVID-19 patients. Yet, extensive validation across diverse datasets and clinical trials is crucial to ensure the robustness and generalizability of these models. The conversation extends into complexities, including ethical considerations around patient privacy and integrating intelligent tech into clinical workflows. Collaborating closely with healthcare professionals ensures this technology complements the established diagnostic approach. Despite the potential to detect COVID-19 using chest X-ray imaging findings, thorough research and validation, alongside ethical deliberations, are vital before implementing it in the healthcare field. The results show that the proposed model achieved classification accuracy and F1 score of 96% and 98%, respectively, for the X-ray images.

This is an open access article under the [CC BY-SA](#) license.



Corresponding Author:

Sivanagireddy Kalli

Department of Electronics and Communication Engineering, Sridevi Women's Engineering College

Hyderabad, Telangana, India

Email: sivanagireddykalli@gmail.com

1. INTRODUCTION

Lung diseases span a vast array of conditions, impacting millions globally. Broadly categorized, they affect lung tissues, blood flow, and airways. Disorders such as asthma, chronic obstructive pulmonary disease (COPD), and pneumonia primarily obstruct airways, impairing the body's oxygen absorption and carbon dioxide expulsion. Blood flow conditions like pulmonary embolism and pulmonary hypertension impede oxygen transport due to arterial clotting in the lungs. Additionally, diseases such as sarcoidosis and pulmonary fibrosis further complicate respiratory health. The COVID-19 pandemic, instigated by the SARS-CoV-2 virus, has heightened global concerns about respiratory health. Common symptoms include dry cough, fatigue, respiratory distress ranging from mild to severe, loss of taste or smell, and fever. The virus

spreads through respiratory droplets expelled when infected individuals sneeze, cough, or talk, posing significant risks to vulnerable populations, including those with underlying health conditions like diabetes, chronic respiratory diseases, cardiovascular disorders, and cancer. Older adults with multiple health issues are particularly susceptible to severe illness from COVID-19.

Diagnostic strategies for COVID-19 encompass antigen tests to detect current infection and antibody tests to ascertain past exposure. Widely used PCR tests detect viral RNA from nasopharyngeal swabs with high accuracy. However, global containment efforts face challenges due to limited testing capacities, uneven resource distribution, and the absence of universally available vaccines or specific treatments. In diagnosing COVID-19, medical imaging technologies play a crucial role, especially in rapidly assessing lung abnormalities. CT scans and X-rays capture detailed chest images, with CT scans offering three-dimensional views that enhance visualization of internal organs and precise disease location identification. In contrast, X-rays provide two-dimensional images suitable for examining dense tissues but lack depth perception. Despite the benefits of CT scans, access to high-quality imaging equipment varies globally. Researchers increasingly focus on using chest CT scans to diagnose COVID-19 due to their superior imaging capabilities. However, accurate interpretation requires skilled radiologists to promptly and accurately identify COVID-19-related abnormalities.

To streamline COVID-19 diagnosis and reduce human intervention, researchers develop automated diagnostic models. One innovative approach involves a three-stage methodology incorporating wavelet-enhanced data augmentation, disease detection, and anomaly localization. This approach compensates for limited COVID-19 CT images by pre-processing them using stationary wavelets to enhance features and mitigate over-fitting. Subsequently, each image undergoes transformations like shearing, rotation, and translation for effective dataset augmentation. In the second stage, transfer learning techniques classify CT scans into COVID and non-COVID categories. Models like ResNet50, with additional convolutional layers for enhanced feature extraction, optimize classification accuracy. The best-performing model is selected based on comparisons with benchmark transfer learning models, ensuring robust performance in distinguishing COVID-19-related anomalies from normal lung images. In the final stage, the selected model's feature maps and activation layers detect anomalies within chest CT images of COVID-19-positive patients, facilitating early and accurate clinical intervention. This research aims to evaluate and compare transfer learning models' performance in detecting COVID-19 from CT scans using a limited dataset. Additionally, the study explores innovative data augmentation techniques to enhance feature map interpretability in deeper neural network layers, improving diagnostic accuracy and reliability. Advancements in medical imaging and artificial intelligence hold promise for enhancing COVID-19 diagnosis and management. By leveraging automated diagnostic models and innovative image processing techniques, researchers aim to overcome existing challenges, expedite COVID-19 infection identification from chest CT scans, support timely healthcare interventions, and mitigate the pandemic's impact on global health systems.

2. LITERATURE SURVEY

The COVID-19 pandemic, caused by the SARS-CoV-2 virus, has strained healthcare systems worldwide, necessitating efficient and accurate diagnostic tools. Early and accurate diagnosis is crucial for effective treatment and containment. While RT-PCR tests are the standard, imaging techniques like chest X-rays and CT scans have proven invaluable in diagnosing and monitoring lung abnormalities associated with COVID-19. Recent advancements in deep learning offer promising solutions for automating and enhancing these diagnostic processes [1]. Chest X-rays provide a quick and accessible method for detecting lung abnormalities, although they offer limited depth perception. CT scans, on the other hand, provide detailed three-dimensional images, allowing for a more comprehensive assessment of lung conditions. Studies have shown that CT scans are more sensitive in detecting COVID-19-related lung abnormalities compared to chest X-rays [2]. COVID-19 exhibits distinct imaging features on chest X-rays and CT scans, including ground-glass opacities, consolidation, and bilateral lung involvement. Identifying these features accurately requires skilled radiologists, which can be a bottleneck in areas with limited medical expertise [3]. Convolutional neural networks (CNNs) have revolutionized image analysis by automating feature extraction and classification processes. These networks have shown remarkable success in medical imaging tasks, including disease detection and anomaly localization [4]. Transfer learning involves pre-training a neural network on a large dataset and fine-tuning it on a specific task. This approach is particularly useful in medical imaging, where labeled data is often scarce.

Models like ResNet, VGG, and densely connected convolutional networks (DenseNet) have been effectively employed in transfer learning for COVID-19 detection [5]. Several studies have explored the use of deep learning models for automatic COVID-19 detection from chest X-rays. Apostolopoulos and Mpesiana [6] developed a CNN-based model achieving high accuracy in classifying COVID-19 cases. They used a dataset of chest X-rays including COVID-19, pneumonia, and healthy cases, demonstrating the potential of CNNs in

distinguishing between these conditions. Ozturk *et al.* [7] introduced a deep learning model capable of detecting COVID-19 from chest X-rays with an accuracy of 98.08%. Their approach employed a DarkNet model, highlighting the effectiveness of deep learning architectures in medical image analysis. CT scans offer higher sensitivity and specificity in detecting COVID-19-related lung abnormalities. Wang *et al.* [8] proposed a deep learning model using a dataset of chest CT images to detect COVID-19 with an accuracy of 82.9%. Their model utilized a combination of CNN and long short-term memory (LSTM) networks to capture spatial and temporal features from CT scans. Jaiswal *et al.* [9] employed a transfer learning approach using the VGG16 model, achieving an accuracy of 91% in classifying COVID-19 from chest CT images. Their study demonstrated the importance of data augmentation and preprocessing in enhancing model performance. Comparative studies have shown that combining chest X-rays and CT scans can improve diagnostic accuracy. For instance, Song *et al.* [10] developed a hybrid model integrating features from both imaging modalities, achieving superior performance compared to models using a single modality. Their research emphasizes the potential of multi-modal approaches in medical imaging. A study by Yan and Liming [11] evaluated chest X-rays' performance in diagnosing COVID-19 and assessed radiologist interpretations' accuracy. The unique CT characteristics of COVID-19 provided crucial insights for healthcare professionals on distinguishing COVID-19 from other viral pneumonias based on imaging findings. The emergence of the novel coronavirus, SARS-CoV-2, underscored the importance of accurate and timely diagnostic imaging in managing global health crisis. Transfer learning has proven effective in addressing the anomaly detection challenge in small medical image datasets, demonstrating promising results in distinguishing COVID-19 cases from other respiratory conditions based on image features. One of main challenges in developing robust deep learning models for COVID-19 detection is scarcity and quality of annotated datasets. Large-scale, diverse datasets are crucial for training models that generalize well across different populations and imaging devices [12].

The well-known Deep CNN establishes the critical benchmarks by Wang *et al.* [8], and Min *et al.* [13] proposed network in network, enhancing CNNs with micro multilayer perceptron (MLP) for improved feature abstraction and classification accuracy. Nishiura *et al.* [14] analyzed COVID-19 serial intervals, providing essential data for transmission modeling and early outbreak response strategies. Images directly obtained from patients suffering with severe COVID-19 or pneumonia are used in this study [15]–[19]. The lack of CT scans with the label "data" in radiology [20]. Additionally, the pretrained CNN model and texture descriptors [21]. The goal of the Imaging COVID-19 AI initiative in Europe [22], [23] and the radiological society of North America (RSNA) [24], [25] is to make data easily accessible to the general public. With the help of these data, different features from different categories can improve interclass variance, which improves deep learning performance. The model will overfit and yield conclusions that are only weakly generalized due to a paucity of data [26], [27]. Therefore, it has been demonstrated that data augmentation works well for training discriminative deep learning models. Flipping, rotating, color jittering, random cropping, elastic distortions, and synthetic data synthesis using generative adversarial networks (GANs) are a few examples of data augmentation techniques [28], [29]. Several visual traits of the medical photos in ImageNet exhibit strong interclass similarity [30], [31]. As a result, conventional augmentation techniques that just make minor image adjustments are less successful [32].

3. PROPOSED METHOD

In medical imaging, deep learning techniques have emerged as powerful tools for automating diagnostics and improving disease detection. Automated COVID-19 diagnosis using medical imaging has been explored using datasets comprising chest X-ray images from patients with bacterial pneumonia, confirmed COVID-19 cases, and uninfected controls. Deep neural network architectures have been investigated to enhance medical image classification accuracy.

DenseNet is a deep learning architecture that was developed to solve some of the shortcomings of CNNs. These problems include vanishing gradients, information loss, and challenges in training extremely deep network. The ability of the DenseNet design to effectively learn from data, eliminate difficulties with vanishing gradients, and achieve great performance with relatively fewer parameters than other architectures has contributed to the rise in popularity of this particular architecture. The number "121" in DenseNet121 refers to the total number of layers, which includes all fully connected, convolutional, pooling, and batch normalization layers. DenseNet121, a CNN architecture, has several notable benefits in diverse computer vision and image analysis applications. One notable benefit is in its extensive connection network, which facilitates the reuse of features and the efficient transmission of information across different layers. In CNNs, the process of combining feature maps is typically performed in a sequential manner. However, DenseNet121 introduces a novel approach where each layer establishes direct connections with all following layers. The high level of connectedness inside the network facilitates the transmission of gradients, mitigates the likelihood of disappearing gradients, and augments the network's total capacity for learning. Consequently,

DenseNet121 has a tendency to need a reduced number of parameters in comparison to other deep designs, making it computationally effective and more amenable to training, especially when confronted with little data. The compact nature of this feature makes it especially advantageous in situations when there are limited processing resources available. One further benefit of DenseNet121 lies in its remarkable efficacy in the processes of feature extraction and representation learning. The network's tight interconnections facilitate the extraction of subtle and highly detailed information from pictures, rendering it particularly advantageous for jobs demanding meticulous analysis, such as image categorization, object recognition, and medical image analysis. Proposed deep learning DenseNet architecture as shown in Figure 1.

In addition, the inclusion of dense skip connections enables the establishment of skip connections across various levels within the network, hence assisting in the retention of low-level characteristics and contextual information over the whole of the network. This approach proves to be very beneficial in the context of tasks such as semantic segmentation, where the availability of pixel-level information is of utmost importance. In several computer vision applications, the popularity and success of DenseNet121 may be attributed to its efficient parameter utilization and feature extraction capabilities. DenseNet121 is an example of a CNN design that has been gaining traction in the world of medical imaging, namely in the identification of COVID-19 utilizing chest X-ray pictures. This is one of the most important applications of this kind of network. The significance of DenseNet121 in the detection of COVID-19 using chest X-ray images lies in the fact that it is able to effectively learn and analyze features from medical images, provide state-of-the-art performance, and ensure data efficiency and interpretability, all of which are essential for accurate and trustworthy disease diagnosis.

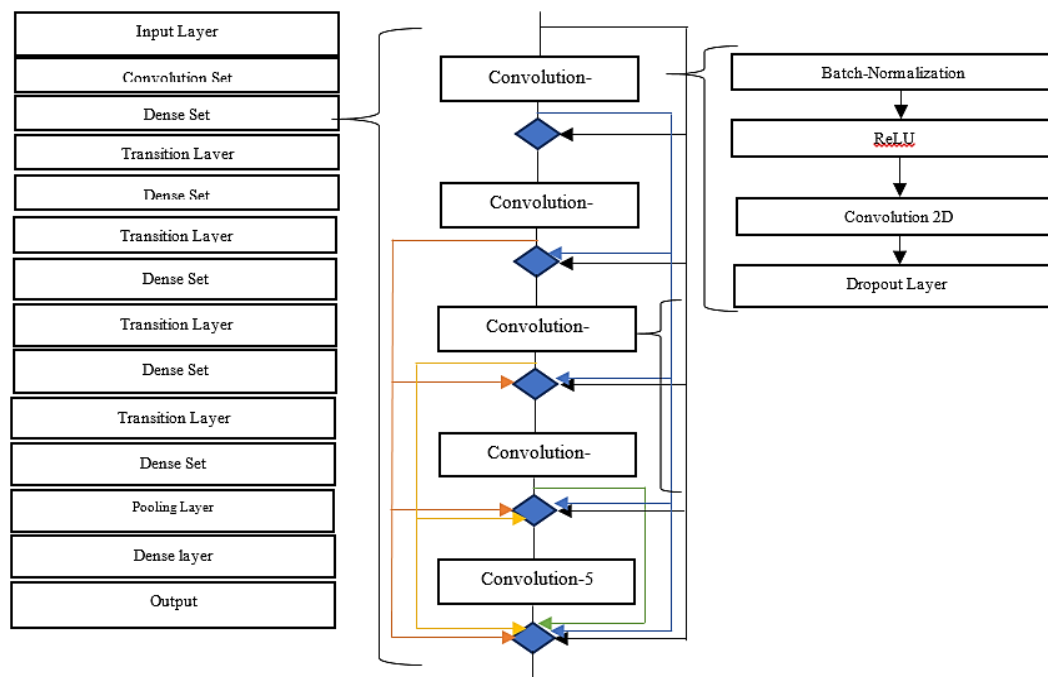


Figure 1. Proposed deep learning DenseNet architecture

4. EXPERIMENTAL RESULTS

In this section, the results of the suggested method are analyzed and examined. Kaggle was the source of the dataset that was used. The dataset was processed using the approach that was proposed. The dataset is structured with three main folders called train, test, and val, and within those three main folders are subfolders labeled "Pneumonia" and "Normal." There are 5,863 X-Ray pictures in the JPEG format, and they are separated into two categories: pneumonia and normal. Chest X-ray pictures were chosen from retrospective cohorts of pediatric patients aged one to five years old at the Guangzhou Women and Children's Medical Center in Guangzhou. The photos were taken in an anterior-posterior orientation. In the course of providing normal clinical treatment for the patients, all chest X-ray imaging was conducted. Before doing the analysis of chest x-ray pictures, every chest radiograph was first subjected to a screening for quality control. This included deleting any scans that were of poor quality or could not be read. After that, the diagnoses for the photos were scored by two highly qualified doctors before being given the green light for use in the

training of the AI system. In order to take into consideration, the possibility of grading mistakes, the assessment set was also reviewed by a third specialist.

The ROC curve is created by comparing the true positive rate (TPR) to the false positive rate (FPR), which is plotted against each other on the x- and y-axes, respectively. Every point on the ROC curve represents a different classification threshold that is applied to the probabilities that are generated by the model. We are able to regulate the balance between sensitivity and specificity by modifying the threshold, and this may be done in accordance with the needs of the issue.

The Figure 2 is a graphical illustration of how well a binary classifier differentiates between the two categories in question. A classifier that achieves high sensitivity (TPR) while simultaneously retaining a low FPR is considered to have greater performance. This is shown by a curve that is closer to the top-left corner. It is common practice to utilize the area under the ROC curve (AUC-ROC) as a summary indicator for the overall performance of the model. A greater capacity for categorization is indicated by an AUC-ROC value that is closer to 1.0. On the ROC graph, the diagonal line at 45 degrees depicts random guessing. This is the case when the TPR and the FPR are identical to one another. A classifier that falls below this diagonal is inferior to random guessing in terms of its predictive power. In contrast, a classifier that is located above the diagonal has some degree of predictive power. The discriminating power of the model increases in proportion to the steepness of the curve's ascent toward the upper left corner. The confusion matrix is a commonly used tabular representation that is utilized to evaluate the efficacy of a classification model.

The assessment of the degree to which a model's predictions correspond with the observed results is an important and useful technique, particularly in scenarios where there is an unequal distribution of classes. In Figure 3, shows the matrix presented seems to pertain to a binary classification task, whereby the classes are denoted as "Normal" and "COVID." The row in question pertains to situations in which the actual class is classified as "Normal." In the present scenario, the model has accurately classified 265 cases as "Normal," but it has made erroneous predictions by classifying 4 instances as "COVID" when they were really "Normal." The term "Actual COVID" refers to cases in which the true class is labeled as "COVID." The model has accurately classified 67 cases as "COVID," but it has made erroneous predictions in 3 instances by classifying them as "Normal" when they were in fact "COVID." The column labeled "Predicted normal" denotes cases that have been classified as "Normal" by the model. Among the occurrences classed as "Normal," a total of 265 were accurately labeled as such, while 3 instances were erroneously classified as "Normal" when they were really cases of "COVID." The column labeled "Predicted COVID" denotes the occurrences that the model has identified and classified as "COVID." Among the occurrences that were categorized as "COVID," a total of 67 instances were accurately labeled as "COVID," whereas 4 instances were erroneously classified as "COVID" when they were really examples of "Normal." The number of instances accurately classified as "COVID" is 67, which are referred to as true positives (TP). True negatives (TN) refer to instances that have been accurately forecasted as "Normal." In this specific case, there are 265 instances that have been properly classified as "Normal." False positives (FP) refer to instances that are incorrectly forecasted as "COVID" when they are really classified as "Normal." In this particular case, there are four instances that fall under this category. False negatives (FN) refer to instances in which the prediction is classified as "Normal," when in reality, it should have been classified as "COVID." In this particular case, there were three instances of FN.

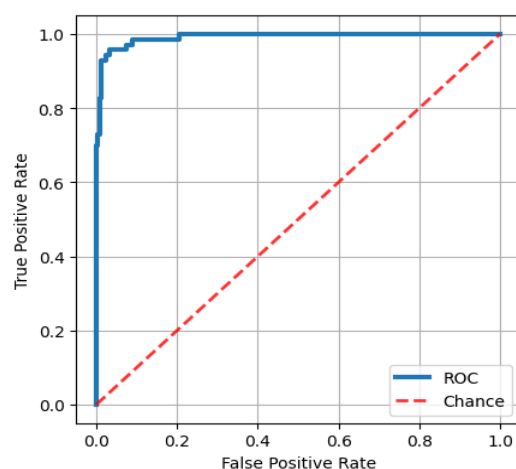


Figure 2. ROC curve

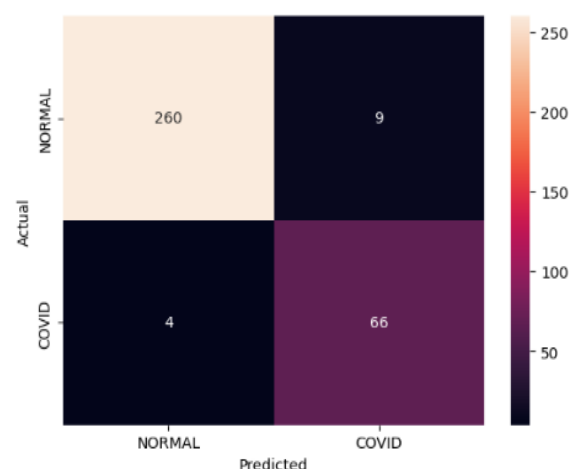


Figure 3. Confusion matrix

The precision-recall curve represented in Figure 4 that visualizes the trade-off between accuracy and recall for various categorization thresholds. It is also known as the precision-recall curve. Predictions are produced using a confidence score or a probability value in many classification algorithms. A threshold is then used to decide whether a prediction is deemed positive or negative. The curve is produced by making small, incremental changes to a predetermined threshold that is used for identifying cases. When the threshold is adjusted, the number of TP, FP, TN, and FN also changes. This, in turn, has an impact on the accuracy and recall of the test. The classifier has a tendency to produce fewer positive predictions when the threshold is set extremely high, which leads to high accuracy but perhaps reduced recall. When the threshold is low, on the other hand, more cases are projected as positive, which increases recall but may result in decreased accuracy.

Figure 5 is F1 score evolution plot which is a statistic that combines accuracy and recall into a single number. This value may be used to evaluate performance. It is especially helpful in situations in which you wish to strike a compromise between the competing values of accuracy and recall. The formula that is used to determine the F1 score is as follows:

$$F1\ Score = 2 \times (Precision \times Recall) / (Precision + Recall)$$

The multiple iterations or different implementations of the categorization model are shown along the x-axis of the Figure 5. Each iteration is a separate effort to enhance the model's functionality in a variety of ways, and these improvements are represented as discrete attempts. The F1 score that the model managed to attain during each iteration is shown along the y-axis. The F1 score is intended to be a measure of the degree to which the model is able to strike a balance between recall and accuracy. When compared to previous scores, a higher F1 score implies improved overall performance. The performance metrics of the proposed model is reported in Table 1.

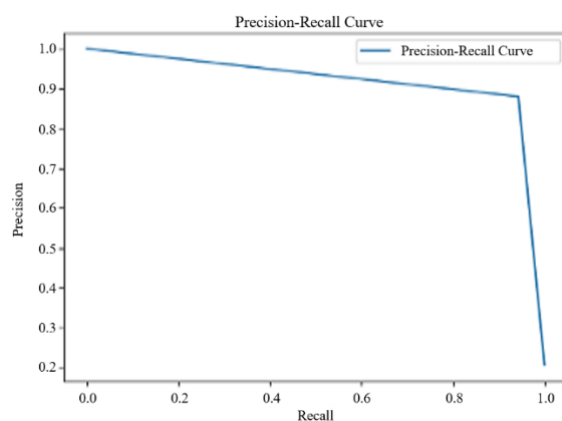


Figure 4. Precision vs recall curve

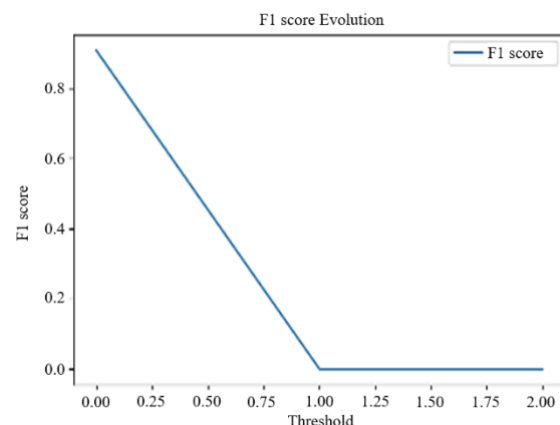


Figure 5. F1 score evolution plot

Table 1. Performance metrics of the proposed model

Label	Precession	Recall	F1 score
Normal	0.98	0.97	0.98
COVID	0.88	0.94	0.91
Accuracy		0.96	

The performance measures that have been presented in Table 1, the efficiency of the model with regard to these important metrics is shown for two separate classes, namely "Normal" and "COVID." An accuracy value of 0.96 is shown by the model when applied to the "Normal" class. This shows that a relatively high percentage of correct positive predictions were made in comparison to the total number of positive predictions made. The fact that the model has a recall value of 0.97 indicates that it is capable of identifying a significant proportion of occurrences that are really positive. A score of 0.98 for the equivalent F1 indicates a balanced performance in terms of both accuracy and recall. In a similar way a precision value of 0.88 for the "COVID" class indicates a satisfactory degree of accuracy in the identification of affirmative cases. The fact that the model was successful in capturing a significant percentage of examples when the hypothesis was correct is shown by the recall value of 0.94. The fact that this specific class has an F1 score of 0.91 indicates that there is a healthy balance existing between accuracy and recall. Comparative results as shown in Table 2.

Table 2. Comparative results

Model	Accuracy (%)
AlexNet	87
VGG16	89
ResNet50	94
Proposed DenseNet model	96

5. CONCLUSION

In conclusion, a classification model was developed in our study to identify COVID-19 cases based on medical image analysis. A dataset comprising both "Normal" and "COVID" cases was utilized, and machine learning techniques were employed to train and evaluate the model's performance. Promising results in terms of accuracy, precision, recall, and F1 score were exhibited by the model. Specifically, an accuracy of 96% was achieved for the "Normal" class, indicating a high percentage of correctly predicted negative cases. The recall of 97% suggested that actual negative cases were proficiently identified, and a well-balanced performance between accuracy and recall was indicated by the F1 score of 98%. For the "COVID" class, a precision of 88% was attained by the model, demonstrating a satisfactory level of accuracy in identifying positive cases. The recall of 94% signified the model's capability to capture a significant proportion of actual positive cases, and the F1 score of 91% confirmed a healthy balance between accuracy and recall for this class. Comparison to other existing models, including AlexNet, VGG16, and ResNet50, was conducted to evaluate our model's performance. Our proposed DenseNet model outperformed these models with an accuracy of 96%, showcasing its effectiveness in the detection of COVID-19 from medical images.

ACKNOWLEDGMENTS

The authors wish to thank ahead of time the Department of Electronics and Communications Engineering and Department of Computer Science and Engineering, Sridevi Women Engineering College, Hyderabad, to assist them in their technical advice and research amenities. We also acknowledge, Dr. A. Narmada, who provided useful comments during model validation.

FUNDING INFORMATION

The study is partially sponsored by the Internal Quality Assurance Cell (IQAC) scheme of the Sridevi Women Engineering College in terms of infrastructure and research facilities. The produced work was not funded by any agency.

AUTHOR CONTRIBUTIONS STATEMENT

This journal uses the Contributor Roles Taxonomy (CRediT) to recognize individual author contributions, reduce authorship disputes, and facilitate collaboration.

Name of Author	C	M	So	Va	Fo	I	R	D	O	E	Vi	Su	P	Fu
Sivanagireddy Kalli	✓	✓	✓	✓	✓	✓	✓	✓	✓	✓	✓	✓	✓	✓
Bukka Narendra Kumar	✓	✓	✓	✓		✓		✓	✓	✓	✓	✓		✓
Saggurthi Jagadeesh	✓	✓	✓	✓		✓	✓	✓	✓	✓	✓		✓	✓
Kushagari Chandramouli Ravi Kumar	✓	✓	✓	✓		✓	✓	✓	✓	✓		✓	✓	✓

C : Conceptualization

M : Methodology

So : Software

Va : Validation

Fo : Formal analysis

I : Investigation

R : Resources

D : Data Curation

O : Writing - Original Draft

E : Writing - Review & Editing

Vi : Visualization

Su : Supervision

P : Project administration

Fu : Funding acquisition

CONFLICT OF INTEREST STATEMENT

The authors indicate that they do not have any known competing financial interests or personal relationships that might have seemed to affect the work reported in this paper. There is no conflict of interest declared by authors.

INFORMED CONSENT

All the people included in this work have signed an informed consent with us. Participants were made to understand what the research involved and their consent was given as per the ethical requirements.

ETHICAL APPROVAL

All the research working with human subjects followed all the necessary national regulations and institutional policies, as well as followed the principles of the Helsinki Declaration. The Institutional Review Board (IRB) of Sridevi Women Engineering College, Hyderabad, Telangana, India. The study is not linked to human subjects or animal research and thus does not need ethical scrutiny.

DATA AVAILABILITY

The data underlying the findings of the present study can be requested by addressing the corresponding author with a reasonable request. The data that was utilized in the research is not openly available or confidential. The data that was utilized in the research is not openly available as per institutional confidentiality policy but can be shared as per reasonable request addressed to the corresponding author.





REFERENCES

- [1] WHO, "Clinical management of severe acute respiratory infection when novel coronavirus (2019-nCoV) infection is suspected: interim guidance," *World Health Organization*, 2020.
- [2] H. Shi *et al.*, "Radiological findings from 81 patients with COVID-19 pneumonia in Wuhan, China: a descriptive study," *The Lancet Infectious Diseases*, vol. 20, no. 4, pp. 425–434, 2020, doi: 10.1016/S1473-3099(20)30086-4.
- [3] A. W. Salehi, P. Baglat, and G. Gupta, "Review on machine and deep learning models for the detection and prediction of Coronavirus," *Materials Today: Proceedings*, vol. 33, pp. 3896–3901, 2020, doi: 10.1016/j.matpr.2020.06.245.
- [4] Y. LeCun, Y. Bengio, and G. Hinton, "Deep learning," *Nature*, vol. 521, no. 7553, pp. 436–444, 2015, doi: 10.1038/nature14539.
- [5] K. He, X. Zhang, S. Ren, and J. Sun, "Deep residual learning for image recognition," in *Proceedings of the IEEE Computer Society Conference on Computer Vision and Pattern Recognition*, 2016, pp. 770–778, doi: 10.1109/CVPR.2016.90.
- [6] I. D. Apostolopoulos and T. A. Mpesiana, "COVID-19: automatic detection from X-ray images utilizing transfer learning with convolutional neural networks," *Physical and Engineering Sciences in Medicine*, vol. 43, no. 2, pp. 635–640, 2020, doi: 10.1007/s13246-020-00865-4.
- [7] T. Ozturk, M. Talo, E. A. Yildirim, U. B. Baloglu, O. Yildirim, and U. Rajendra Acharya, "Automated detection of COVID-19 cases using deep neural networks with X-ray images," *Computers in Biology and Medicine*, vol. 121, 2020, doi: 10.1016/j.compbiomed.2020.103792.
- [8] L. Wang, Z. Q. Lin, and A. Wong, "COVID-Net: a tailored deep convolutional neural network design for detection of COVID-19 cases from chest X-ray images," *Scientific Reports*, vol. 10, no. 1, Nov. 2020, doi: 10.1038/s41598-020-76550-z.
- [9] A. Jaiswal, N. Gianchandani, D. Singh, V. Kumar, and M. Kaur, "Classification of the COVID-19 infected patients using DenseNet201 based deep transfer learning," *Journal of Biomolecular Structure and Dynamics*, vol. 39, no. 15, pp. 5682–5689, 2021, doi: 10.1080/07391102.2020.1788642.
- [10] Y. Song *et al.*, "Deep learning enables accurate diagnosis of novel coronavirus (COVID-19) with CT images," *IEEE/ACM Transactions on Computational Biology and Bioinformatics*, vol. 18, no. 6, pp. 2775–2780, 2021, doi: 10.1109/TCBB.2021.3065361.
- [11] L. Yan and X. Liming, "Coronavirus disease 2019 (COVID-19): role of chest CT in diagnosis and management," *American Journal of Roentgenology*, vol. 214, no. 6, pp. 1280–1286, 2020.
- [12] P. Zhou *et al.*, "A pneumonia outbreak associated with a new coronavirus of probable bat origin," *Nature*, vol. 579, no. 7798, pp. 270–273, 2020, doi: 10.1038/s41586-020-2012-7.
- [13] L. Min, C. Qiang, and Y. Shuicheng, "Network in network," in *2nd International Conference on Learning Representations, ICLR 2014 - Conference Track Proceedings*, 2014.
- [14] H. Nishiura, N. M. Linton, and A. R. Akhmetzhanov, "Serial interval of novel coronavirus (COVID-19) infections," *International Journal of Infectious Diseases*, vol. 93, pp. 284–286, 2020, doi: 10.1016/j.ijid.2020.02.060.
- [15] M. Turkoglu, "COVIDetectionNet: COVID-19 diagnosis system based on X-ray images using features selected from pre-learned deep features ensemble," *Applied Intelligence*, vol. 51, no. 3, pp. 1213–1226, 2021.
- [16] A. A. Ardakani, A. R. Kanafi, U. R. Acharya, N. Khadem, and A. Mohammadi, "Application of deep learning technique to manage COVID-19 in routine clinical practice using CT images: results of 10 convolutional neural networks," *Computers in Biology and Medicine*, vol. 121, 2020, doi: 10.1016/j.compbiomed.2020.103795.
- [17] L. Brunese, F. Mercaldo, A. Reginelli, and A. Santone, "Explainable deep learning for pulmonary disease and coronavirus COVID-19 detection from X-rays," *Computer methods and programs in biomedicine*, vol. 196, 2020, doi: 10.1016/j.cmpb.2020.105608.
- [18] Y. Chen, Q. Liu, and D. Guo, "Emerging coronaviruses: Genome structure, replication, and pathogenesis," *Journal of Medical Virology*, vol. 92, no. 4, pp. 418–423, 2020, doi: 10.1002/jmv.25681.
- [19] S. B. Stoecklin *et al.*, "First cases of coronavirus disease 2019 (COVID-19) in France: surveillance, investigations and control measures, January 2020," *Eurosurveillance*, vol. 25, no. 6, 2020, doi: 10.2807/1560-7917.ES.2020.25.6.2000094.
- [20] D. P. Fan *et al.*, "Inf-Net: automatic COVID-19 lung infection segmentation from CT images," *IEEE Transactions on Medical Imaging*, vol. 39, no. 8, pp. 2626–2637, 2020, doi: 10.1109/TMI.2020.2996645.
- [21] R. M. Pereira, D. Bertolini, L. O. Teixeira, C. N. Silla, and Y. M. G. Costa, "COVID-19 identification in chest X-ray images on flat and hierarchical classification scenarios," *Computer Methods and Programs in Biomedicine*, vol. 194, 2020, doi: 10.1016/j.cmpb.2020.105532.
- [22] EusoMII, "A European initiative for automated diagnosis and quantitative analysis of COVID-19 on imaging," *EusoMII*, 2020. [Online]. Available: <https://www.eusomii.org/a-european-initiative-for-automated-diagnosis-and-quantitative-analysis-of-covid-19-on-imaging/>
- [23] N. Zhang *et al.*, "Recent advances in the detection of respiratory virus infection in humans," *Journal of Medical Virology*, vol. 92, no. 4, pp. 408–417, 2020, doi: 10.1002/jmv.25674.





- [24] RSNA, "RSNA announces COVID-19 imaging data repository," *Radiological Society of North America*, 2021. [Online]. Available: <https://www.rsna.org/news/2020/march/covid-19-imaging-data-repository>
- [25] V. M. Corman *et al.*, "Detection of 2019 novel coronavirus (2019-nCoV) by real-time RT-PCR," *Eurosurveillance*, vol. 25, no. 3, 2020, doi: 10.2807/1560-7917.ES.2020.25.3.2000045.
- [26] J. Wang and L. Perez, "The effectiveness of data augmentation in image classification using deep learning," *arXiv-Computer Science*, pp. 1-8, 2017.
- [27] P. Yadav, N. Menon, V. Ravi, and S. Vishvanathan, "Lung-GANs: unsupervised representation learning for lung disease classification using chest CT and X-ray images," *IEEE Transactions on Engineering Management*, vol. 70, no. 8, pp. 2774–2786, 2023, doi: 10.1109/TEM.2021.3103334.
- [28] J. Deng, W. Dong, R. Socher, L. J. Li, K. Li, and L. Fei-Fei, "ImageNet: a large-scale hierarchical image database," in *2009 IEEE Conference on Computer Vision and Pattern Recognition, CVPR 2009*, 2009, pp. 248–255, doi: 10.1109/CVPR.2009.5206848.
- [29] A. Arunachalam, V. Ravi, V. Acharya, and T. D. Pham, "Toward data-model-agnostic autonomous machine-generated data labeling and annotation platform: COVID-19 autoannotation use case," *IEEE Transactions on Engineering Management*, vol. 70, no. 8, pp. 2695–2706, 2023, doi: 10.1109/TEM.2021.3094544.
- [30] A. Ben-Cohen, E. Klang, M. M. Amitai, J. Goldberger, and H. Greenspan, "Anatomical data augmentation for CNN based pixel-wise classification," in *2018 IEEE 15th International Symposium on Biomedical Imaging (ISBI 2018)*, 2018, pp. 1096–1099, doi: 10.1109/ISBI.2018.8363762.
- [31] D. Mukhtorov, M. Rakhmonova, S. Muksimova, and Y. I. Cho, "Endoscopic image classification based on explainable deep learning," *Sensors*, vol. 23, no. 6, 2023, doi: 10.3390/s23063176.
- [32] C. I. Paules, H. D. Marston, and A. S. Fauci, "Coronavirus infections more than just the common cold," *JAMA-Journal of the American Medical Association*, vol. 323, no. 8, pp. 707–708, 2020, doi: 10.1001/jama.2020.0757.

BIOGRAPHIES OF AUTHORS







Sivanagireddy Kalli     is presently a Professor of Electronics and Communication Engineering. He did his Ph.D. degree in Electronics and Communication Engineering from JNTU Hyderabad in 2019. He is having more than 22 years of teaching and 8 years of research experience. He has a total of 60 research publications in international journals and 9 patents. His current research areas are artificial intelligence, machine learning, and deep learning. He is a member of IEEE. He can be contacted at email: sivanagireddykalli@gmail.com.







Bukka Narendra Kumar     is presently a Professor of Computer Science and Engineering and HoD. He did his Ph.D. degree in Computer Science and Engineering from JNTU Hyderabad in 2019. He is having more than 25 years of teaching and 8 years of research experience. He has a total of 20 research publications in international journals and 4 patents. His current research areas are information security, artificial intelligence, machine learning, and deep learning. He is a life member of MISTE. He can be contacted at email: bnkphd@gmail.com.



Saggurthi Jagadeesh     is presently Professor of Electronics and Communication Engineering. He did his Ph.D. degree in Electronics and Communication Engineering from JNTU Hyderabad in 2019. He is having more than 25 years of Teaching and 8 years of research experience. He has a total of 40 research publications in international journals and 9 patents. His current research areas are artificial intelligence, machine learning, and deep learning. He is a member of IEEE. He can be contacted at email: jaaga.ssjec@gmail.com.



Kushagari Chandramouli Ravi Kumar     is presently Professor of Computer Science and Engineering. He did his Ph.D. degree in Computer Science and Engineering from JNTU Hyderabad in 2019. He is having more than 29 years of teaching and 8 years of research experience. He has a total of 20 research publications in international journals and 3 patents. His current research areas are artificial intelligence, machine learning, and deep learning. He is a member of MISTE. He can be contacted at email: kcravikunar1971@gmail.com.